NUCLEAR INSTRUMENTS AND METHODS 95 (1971) 563–569; © NORTH-HOLLAND PUBLISHING CO.

AN ABSOLUTE MEASUREMENT OF THE EFFICIENCY OF A BF_3 PROPORTIONAL COUNTER

T. E. SAMPSON* and D. H. VINCENT

Department of Nuclear Engineering, The University of Michigan, Ann Arbor, Michigan, U.S.A.

Received 8 April 1971

We report an absolute measurement of the efficiency of a BF_3 counter in narrow beam geometry in the energy range from 0.024 eV to 0.111 eV. Agreement with calculated efficiency values is excellent. No significant end effects are noted. The basic feature of this experiment is the measurement of the incident neutron flux by gold foil activation and counting in an NaI well counter which was calibrated with gold foils irradiated in the National Bureau of Standards Standard Thermal Neutron Flux.

1. Introduction

Boron trifluoride (BF_3) counters utilizing the $^{10}B(n,\alpha)^7Li$ reaction are one of the most widely used thermal neutron detectors. Their utility is enhanced by the fact that it is possible to calculate their efficiency for many experimental situations.

For the idealized case of a narrow collimated neutron beam directed parallel to the axis of a cylindrical BF_3 counter with negligibly thin end window, the expression for the efficiency is well known. See ref. 1 for example.

$$\varepsilon(E) = 1 - \exp\left[-\Sigma_a(E)\,L\right] . \qquad (1)$$

Here $\varepsilon(E)$ is the detector efficiency at energy E, $\Sigma_a(E)$ is the macroscopic absorption cross section of the ^{10}B isotope in the counter and L is the active length of the counter. Implicit in this expression are the assumptions that the neutron absorption by ^{10}B is the only neutron interaction in the counter and that all absorptions are counted.

In practice these assumptions are not valid. Interactions in the end window (or counter walls for side incidence) must be considered and all possible neutron interactions with all fill gas constituents must be taken into account. Many counters contain a "dead space" between the end window and the active volume and a similar region at the rear of the active volume. Neutron interactions in these regions are not detected. However, interactions near the boundaries of these dead spaces may result in partial energy deposition in the active volume. Partial energy deposition will also result from absorptions near the counter walls when one of the reaction products strikes the walls. The number of these partial energy deposition events (end and wall effects) that are counted depends upon the discriminator bias of the associated counting circuitry and thus affects the counter efficiency.

Fowler and Tunnicliffe[2]) discuss these effects in detail and also describe their effect on the determination of counter efficiency. For low efficiency counters a correction to the geometrical length of the active volume arising from end effects may be determined by comparing the count rates of two counters of different lengths, but otherwise identical construction[2]).

End and wall effects and the fact that the idealizing assumptions of eq. (1) are not valid make an independent measurement of counter efficiency desirable. Such a measurement, besides providing an absolutely calibrated detector, can also yield information on the magnitude of end or wall effects and end window and dead space transmission corrections. In the following, we will discuss such an independent absolute efficiency measurement and compare the measurement with a more rigorous calculated efficiency than eq. (1).

2. Outline of experiment

The BF_3 counter efficiency was measured using a narrow monoenergetic neutron beam from a thermal neutron crystal spectrometer. The 0.635 cm diam. neutron beam was incident on the center of the 5.08 cm diam. counter end window directed parallel to the counter axis.

The monoenergetic neutron flux was measured by counting the activity of gold foils irradiated in the incident beam. These foils were counted in an NaI(Tl) well counter whose efficiency had been previously measured by counting identical foils which had been irradiated in the National Bureau of Standards Standard Thermal Neutron Flux.

* Present address: Los Alamos Scientific Laboratory, Los Alamos, New Mexico, U.S.A.

3. BF_3 counter characteristics

The BF_3 counter used was chosen to minimize the previously discussed effects that add uncertainties to the calculated detector efficiency.

A ceramic end window counter with the anode imbedded directly in the end window was chosen. This eliminates the complications of dead space and ensures a uniform efficiency across the end window, since the usual insulator and its attendant neutron absorption is eliminated. Detectors of this type are commonly used in neutron diffraction spectrometers. The 5.08 cm diam. chosen was thought to be sufficiently large to minimize neutron interactions near the walls when used with a 0.635 cm diam. beam. Since the pulse height resolution generally worsens as the counter diameter increases, it was not thought desirable to use a counter larger than 5.08 cm diam.

A low efficiency counter was chosen to minimize dead time corrections (approximately 10% efficiency at 0.035 eV). The maximum neutron flux of $\approx 10^4 n/cm^2$-sec in the 0.635 cm diam. beam would produce a count rate on the order of 300 counts/sec in this counter. For an assumed dead time of 10 μsec this would result in a 0.3% dead time correction. This correction was not made to the data, but was included in the uncertainty of the final result.

Several combinations of filling gas enrichment and pressure were possible to attain this efficiency. A high total filling pressure in the counter was desired to reduce wall effects by minimizing the range of the ^7Li and α particle reaction products. To attain this dual requirement of low efficiency and high total filling pressure the fill gas was specified to be 46 cm Hg of argon and 30 cm Hg of depleted BF_3 ($\approx 11\%$ ^{10}B). For this mixture an empirical formula[1]) gives the range of the 1.47 MeV α particles produced in 93.6% of the interactions as 0.74 cm. Complete detector specifications are listed in table 1.

TABLE 1

BF_3 counter specifications.

Manufacturer:	Reuter-Stokes Electronic Components, Inc., Cleveland, Ohio, U.S.A.
Model:	RSN-108S-MG proportional counter ceramic end window thermal neutron detector Serial No. F2169
Diameter:	5.08 cm
Active length:	32.38 cm
Outer shell:	304SS, 0.089 cm thick
Anode:	0.005 cm diam. tungsten
End window:	0.203 cm thick alumina ceramic (Al_2O_3)
Fill gas:	46 cm Hg argon 30 cm Hg depleted BF_3 (10.91 % ^{10}B)

The BF_3 counter was operated at 2150 V and exhibited a flat plateau from 1950 V to above 2500 V. Typical pulse height distributions are shown in fig. 1. The change in the spectrum from increased wall effects due to the broad beam geometry is particularly evident in fig. 1b. The efficiency measurements were carried out in the narrow beam geometry that produced the pulse height distribution of fig. 1a.

The flatness of the detector response as a function of radial beam position is verified in fig. 2. No deviation from uniform response is observed near the anode.

4. Well counter calibration

An absolute measurement of a BF_3 counter efficiency requires an absolute measurement of the neutron flux incident on the counter. In these measurements the monoenergetic neutron flux was determined by counting the activity of gold foils irradiated in the beam entering the counter.

4.1. Flux foil and foil counter

The principle reason for using gold foils was that the National Bureau of Standards (NBS) Standard

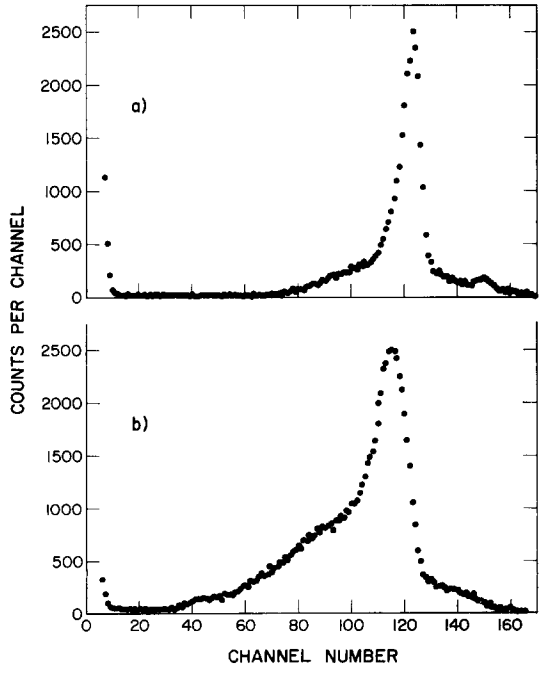

Fig. 1. BF_3 counter pulse height distributions. a) 0.635 cm diam. beam parallel to counter axis at counter center; b) large diameter beam parallel to counter axis, end window fully illuminated.

Thermal Neutron Flux had been calibrated using gold foils[3]). It was felt that this facility would enable one to obtain gold foils of accurately known activity for counter calibration. Gold foils are also convenient because the absorption cross section of gold is well known and widely used as a standard cross section. Also, 95.7%[4]) of its decays produce a 411.8 keV gamma ray which is easily counted. One disadvantage is that its long half life of 2.698 days[4]) necessitates long irradiations to approach saturation.

A thick foil would maximize activity yet it was believed desirable to keep the foil nearly the same thickness as those used to calibrate the NBS standard flux (0.025 mm and 0.00635 mm) in order that cadmium ratio and self-shielding corrections would be of the same magnitude as those used in the NBS flux measurement. A compromise foil thickness of 0.127 mm was chosen. A 0.635 cm diam. foil of 0.127 mm thickness ($\approx$ 75 mg) yields a saturation activity of 230 dis/sec for a 10^4 n/cm^{2}sec flux of 2200 m/sec neutrons. It would require an irradiation of over nine days to approach this activity. This meant that a high efficiency counter was needed to count the gold activity.

Four pi beta counting was ruled out because of the large and inadequately known corrections for self-absorption and self-scattering which are necessary for thick foils.

The highest efficiency detector conveniently available for gamma counting was an NaI(Tl) well crystal.

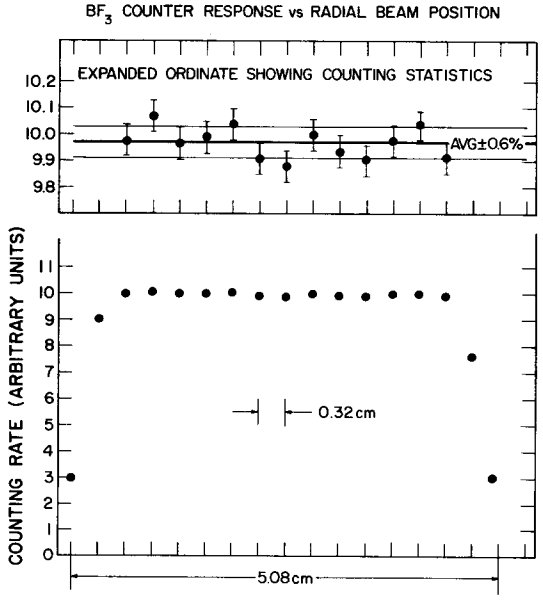

Fig. 2. BF_3 counter response vs radial beam position for 0.635 cm diam. beam incident on end window parallel to counter axis.

Calculations by Snyder[5]) indicate absolute total efficiencies ranging from about 0.40 to 0.50 for a 5.08 cm $\times$ 5.08 cm well crystal of this type depending upon the source geometry. Snyder's calculations also indicate that these counters are insensitive to small changes in source geometry inside the well. This is desirable since it reduces the problem of exact reproducibility of geometry between measurements. The well crystal used was a Harshaw Integral Line Type 8SF8. The 5.08 cm diam. $\times$ 5.08 cm thick crystal had a 2.86 cm diam. by 3.81 cm deep well. The crystal was canned in 0.038 cm thick aluminum and mounted on a 5.08 cm diam. Dumont 6292 photomultiplier. The counting electronics consisted of a linear amplifier, integral discriminator, and scaler.

The foils were placed in the bottom of a pyrex test tube inserted in the well. The 400 mg/cm^2 wall thickness of the test tube plus the 100 mg/cm^2 thickness of the aluminum crystal canning was more than enough to absorb all the 0.96 MeV betas produced in the decay of ^{198}Au. This ensured that only gammas were counted by the well crystal.

4.2. NBS STANDARD FLUX MEASUREMENT

A discussion of the analysis and corrections applied in the calibration of the NBS standard thermal neutron flux[3]) is desirable in order to understand the well counter calibration. This is important since different size foils were used to calibrate the well counter than were used in the NBS flux measurement.

Mosburg and Murphy[3]) used beta-gamma coincidence counting to determine the absolute activity of 0.0254 mm and 0.00635 mm thick gold foils irradiated in the NBS standard flux. They corrected the observed activity for the contribution from epithermal neutrons. The cadmium ratio defined as

$$R_{Cd} = \frac{\text{bare foil activity}}{\text{Cd covered foil activity}}$$

was measured with 0.102 cm thick cadmium. The Cd covered activity was also corrected for shielding of the epithermal flux by the Cd.

Since neutron absorption in the outer layers of the foil reduces the flux at the center of the foil it was necessary to make a self-shielding correction. The correction used was that derived by Bothe[6]) for a mono-energetic isotopic flux. Flux depression at the foil surface was neglected since the irradiations were carried out in an air filled cavity.

A correction for internal conversion in the decay scheme of ^{198}Hg was also made. This correction was

not straightforward because the effects of conversion electron detection had to be considered in the beta-gamma coincidence measurements.

The NBS standard flux in terms of these measurements is given by

$$\varphi_{\mathrm{NBS}}^{\mathrm{thermal}} = \frac{A_\infty F_{\mathrm{NBS}}}{N_{\mathrm{T}} \sigma_0 G_{\mathrm{NBS}} H_{\mathrm{NBS}}}, \qquad (2)$$

where A_∞ is the saturation disintegration rate; N_{T} is the number of ^{197}Au atoms in the foil; σ_0 is the 2200 m/sec absorption cross section of ^{197}Au ($98.8 \pm \pm 0.3$ b); G_{NBS} is the self-shielding correction; H_{NBS} is the internal conversion correction; and F_{NBS} is the cadmium ratio correction.

It is noted that the 2200 m/sec absorption cross section of ^{197}Au is used in computing the thermal flux. An average cross section for a Maxwellian is not used nor is the Maxwellian temperature mentioned. Thus $\varphi_{\mathrm{NBS}}^{\mathrm{thermal}}$ is a defined thermal flux which may or may not be equal to the absolute thermal flux in the NBS standard pile. Nevertheless the correct disintegration rate for a foil irradiated in this flux can be calculated if the corrections discussed above are applied.

4.3. Well counter efficiency

Two 0.635 cm diam. by 0.127 mm thick ^{197}Au foils were irradiated to $\approx 87\%$ of saturation in the NBS standard thermal neutron flux and then counted in the well counter described previously. Solving eq. (2) for the saturation activity gives

$$D_0 = N_{\mathrm{T}} \sigma_0 \varphi_{\mathrm{NBS}}^{\mathrm{thermal}} G(1/F) H, \qquad (3)$$

where D_0 denotes the saturation activity and the unsubscripted corrections G, F and H refer to our foils. The self-shielding correction, G, was calculated to be 0.902. The Cd ratio, furnished as a function of foil thickness by the NBS, was 12.8 for our 0.127 mm thick foils leading to a value of 0.9219 for F. The decay scheme correction, H, for our foils was calculated from the decay scheme[4]) to be 0.9588. This is the fraction of all ^{198}Au decays that give rise to a gamma ray. This correction neglected the 0.025% of the betas that lead to the ground state of ^{198}Hg and also neglected internal conversion of the 1.087 MeV level of ^{198}Hg which is populated in only 1% of the decays. The magnitude of $\varphi_{\mathrm{NBS}}^{\mathrm{thermal}}$ at the time of our foil irradiations was $4254 \pm 1.5\%$ n/cm^{2}sec.

The observed well counter count rate was corrected for the gold activity decay and compared to the foil disintegration rate from eq. (3). This led to a well counter efficiency of $\varepsilon_{\mathrm{well}} = 0.429 \pm 0.007$ (1.6%), the major source of error being the quoted $\pm 1.5\%$ error in $\varphi_{\mathrm{NBS}}^{\mathrm{thermal}}$.

It is noted that the self-shielding correction G was derived for a monoenergetic isotropic flux. A more valid correction may be that quoted by Hanna[7]) for a Maxwellian flux distribution. However, it is found that the ratio $G_{\mathrm{Max}}/G_{\mathrm{mono}}$ for the 0.0254 mm foils used by Mosburg and Murphy is nearly identical to that for our 0.127 mm foils. Thus the monoenergetic flux assumption does not introduce any additional error into the activity of our foils due to the difference in thickness.

During the well counter calibration a standard ^{137}Cs source was also counted to serve as a reference to determine efficiency drifts over long periods of time.

5. BF_3 counter efficiency measurement

The BF_3 counter efficiency measurements were carried out in a monoenergetic neutron beam from a crystal spectrometer at the University of Michigan Ford Nuclear Reactor. The BF_3 counter was housed in a cylindrical borated paraffin shield and was connected to standard counting electronics consisting of a preamplifier, linear amplifier and integral discriminator, and scaler. A 1.27 cm thick Benelex disc covered with 0.51 mm of cadmium on both sides was placed over the end of the shield directly in front of the counter. A 0.635 cm diam. hole in the Cd covered Benelex allowed a narrow beam to be incident on the center of the counter end window. The gold foil was fitted into the Cd on the rear (BF_3 counter side) of the Benelex disc.

This arrangement was irradiated in the spectrometer beam for times varying from 38 h to 67 h depending upon the beam flux and energy. During the irradiation the neutron beam transmitted through the gold foil was counted with the BF_3 counter. Approximately twenty 10 min counts were taken during the course of each irradiation.

Measurements were made at eight energies between 0.024 eV and 0.111 eV. At each energy the second order contamination in the beam was measured by observing the transmission of a 0.152 cm thick ^{197}Au sample.

For each run the gold foil activity was counted in the calibrated well counter. The well counter efficiency was corrected for drift (typically $\approx 2\%$) by counting the standard ^{137}Cs source.

A correction for parallel beam self-shielding ($\approx 2-4\%$) was made and after making the decay scheme correction the saturation activity A_∞^0 was used

to calculate the neutron flux φ_0 incident on the foil from

$$\varphi_0 = A^0_\infty / N_T \sigma_a(E) . \quad (4)$$

The total number of atoms in the foil, N_T, was obtained by weighing the foil. The absorption cross section of ^{197}Au, $\sigma_a(E)$, was calculated for each energy.

It is desirable to calculate $\sigma_a(E)$ [8]) because of uncertainties in subtracting the scattering cross section from the total cross section to obtain $\sigma_a(E)$. Also $\sigma_a(E)$ is not exactly proportional to $1/v$ because of the large resonance at 4.91 eV. At energies below 4.91 eV, $\sigma_a(E)$ can be divided into two parts, a $1/v$ part and a portion arising from the wings of the resonance. The resonance contribution is calculated from Breit-Wigner formula[8]) and added to the $1/v$ contribution. At 2200 m/s the $1/v$ and resonance contributions are 97.7 and 1.1 b respectively.

The average BF_3 counter count rate recorded during the irradiation was corrected for transmission through the gold foil to obtain the open beam count rate. This open beam count rate, R_0, is expressed in terms of the counter efficiency ε_{BF_3} and neutron flux by

$$R_0 = \varepsilon_{BF_3} \varphi_0 a , \quad (5)$$

where a is the cross sectional area of the 0.635 cm diam. neutron beam. Combining eqs. (4) and (5) after correcting R_0 and A^0_∞ for background gives the BF_3 counter efficiency

$$\varepsilon_{BF_3}(E) = R_0 N_T \sigma_a(E) / A^0_\infty a . \quad (6)$$

This assumes that the neutron beam contains no second-order contamination. An expression for the BF_3 counter efficiency taking second-order contamination into account has been derived[9]),

$$\varepsilon_{BF_3}(E) = \frac{R_0 N_T [\sigma_a(E) + \alpha \sigma_a(4E)]}{A^0_\infty a} - \alpha \varepsilon_{BF_3}(4E) . \quad (7)$$

Here α is the ratio of the second-order to first-order flux in the beam. To compute the counter efficiency at energy E the efficiency at the second-order energy, $4E$, must be known. With very little error $\varepsilon_{BF_3}(4E)$ may be replaced by its calculated value if the efficiency has not been measured at $4E$. The calculated BF_3 counter efficiency at energy $4E$ was used in all data reduction concerning second-order effects.

Second-order contamination was found to be greater than a few percent only for the data points at 0.033 eV and 0.024 eV. Even for those points the difference in counter efficiency calculated from eq. (6) and eq. (7) was negligible.

The background corrections to R_0 and A^0_∞ mentioned previously were measured by moving the monochromating crystal 2° off the Bragg condition. These measurements coupled with measurements taken with Cd and/or additional fast-neutron shielding in the beam indicated that 50% of the background in BF_3 counter came from incoherently scattered thermal neutrons in the 0.635 cm beam and 40% arose from fast neutrons in the narrow beam and those penetrating the Cd covered masonite shield. The background contribution of these neutrons to the gold foil activity was estimated as follows: An average for all data points showed the ratio of the absorption efficiencies of the gold foil and the BF_3 counter to be ≈ 0.63. The gold foil will "see" all the incoherently scattered thermal neutrons in the narrow beam but will "see" only a fraction of the fast neutron background seen by the BF_3 counter. This fraction was somewhat arbitrarily estimated at $\frac{1}{2}$. Thus the gold foil will see $50\% + \frac{1}{2}$ (40%) or 70% of the background neutrons seen by the BF_3 counter. But it "sees" this background with a relative efficiency of only 0.63 of that of the BF_3 counter. Thus the foil sees 0.45 of the percentage background that the BF_3 counter sees. Typical results for this correction were: Total BF_3 counter background ≈ 250 counts/min $\approx 2\%$ correction in R_0. This resulted in a 0.9% correction in A^0_∞. The net effect on ε_{BF_3} was 1.0 – 1.5% for most points.

6. Ideal BF_3 counter efficiency

An idealized expression for the efficiency of a BF_3 counter in a narrow beam parallel to the detector axis has been given in eq. (1). In practice one must include the effects of end window transmission and all interactions in the filling gas. When this is done eq. (1) takes the form

$$\varepsilon_{BF_3}(E) = \exp(-\Sigma^W_T(E) X_W) (\Sigma^{10B}_a(E)/\Sigma_T(E)) \times \times [1 - \exp(-\Sigma_T(E) L)]. \quad (8)$$

Here $\Sigma^W_T(E)$ is the macroscopic total cross section of the end window, X_W is the end window thickness, L is the length of the active volume of the counter and

$$\Sigma_T(E) = \Sigma^{10B}_a(E) + \Sigma^{10B}_S(E) + \Sigma^A_T(E) + \Sigma^{11B}_T(E) + \Sigma^F_T(E) , \quad (9)$$

where the subscripts T, S and a refer to the macroscopic total, scattering and absorption cross sections of the boron isotopes, argon and fluorine in the counter.

Here the end window transmission correction has been somewhat simplified since a small angle scattering event has a reduced, but still finite probability of being detected as it may traverse a short segment of the active volume. This effect is small and has been neglected.

The counter efficiency was calculated from eq. (8) using cross sections from BNL-325. The ^{10}B absorption cross section was taken to be exactly proportional to $1/v$ with σ_a (2200 m/sec) = 3837 b.

The filling gas density was calculated assuming the counter was filled at 20 °C and that the fill gas behaved as an ideal gas. The manufacturer claimed an error of less than 0.25% on the fill pressure. The manufacturer also verified that the fill pressures were measured at room temperature and not corrected to STP. This is an important point to verify for measurements of this type since one might be misled by textbook examples[1]) which assume STP filling conditions. Indeed, if the counter efficiency is calculated assuming STP filling conditions, taking end window transmission into account, but neglecting all interactions except ^{10}B absorption in the active volume, one obtains a calculated efficiency that is systematically $\approx 8\%$ higher than the measured values. The major portion of this discrepency is due to the incorrect fill temperature-pressure assumption.

7. Results

The measured BF_3 counter efficiency is shown in fig. 3 along with the calculated efficiency from eq. (8). The agreement is seen to be excellent. A least squares fit to the measured points yields the expression

$$\varepsilon_{BF_3}(E) = 0.592 + 1.744\,E^{-\frac{1}{2}}\,, \qquad (10)$$

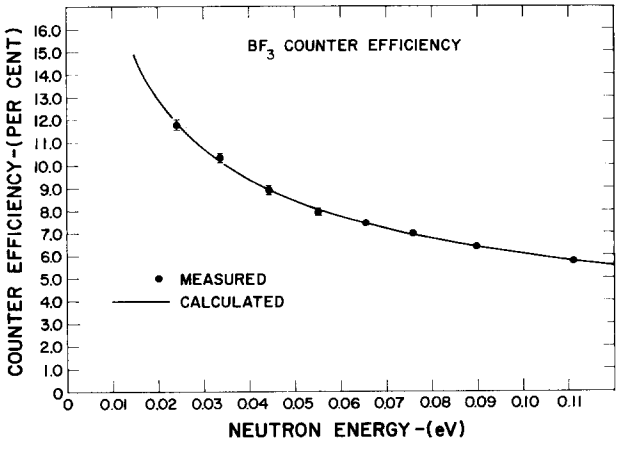

Fig. 3. Measured and calculated BF_3 counter efficiency. ●● – measured; ——— calculated from eq. (8).

where ε is in percent and E is in eV. This curve (not plotted) is indistinguishable from the calculated efficiency curve [eq. (8)] shown in fig. 3.

8. Experimental errors

Errors can be assigned to all of the factors in eq. (6) used to calculate the BF_3 counter efficiency. Uncertainties in R_0 arise from counting statistics, 0.10% typically, and reactor power level fluctuations during the irradiation, 0.30% estimated from the variation of the BF_3 count rate with time, this variation being greater than that expected from counting statistics alone. These independent contributions yield an uncertainty of 0.32% in R_0. No error is assigned to the foil transmission correction since in the entire error propagation small errors in small corrections are neglected.

An uncertainty of 0.14% in N_T was estimated from the reproducibility of foil weights.

The error in the ^{197}Au absorption cross section is 0.3% while the 1.6% uncertainty in A_∞^0 arises from the 1.6% error in ε_{well}. Errors arising from the self-shielding and decay scheme correction applied to A_∞^0 are neglected.

An 0.80% error is assigned to the beam area a which arises from an estimated 0.0025 cm uncertainty in the diameter of the aperture placed before the counter.

An assumed 10 μsec dead time for BF_3 counter results in a 0.20% correction which is assumed to contribute to the uncertainty in ε_{BF_3}.

The background correction discussed in section 5 is assigned an error of 0.3%.

Assuming the above errors are independent, their quadratic sum yields a final uncertainty in ε_{BF_3} of $\pm$ 1.9%. The error bars in fig. 3 represent this uncertainty.

9. Conclusions

We have made careful measurements of the efficiency of a BF_3 counter in narrow beam geometry in the energy range from 0.024 eV to 0.111 eV. The measured efficiency is in excellent agreement with calculated values when one includes the effects of end window transmission and all interactions in the filling gas. End effects are not observed in this low efficiency counter within the accuracy of the experiment ($\pm$2%).

These measurements give confidence that BF_3 counter efficiencies can be calculated to good accuracy if one has access to accurate filling pressure and temperature data and if one includes all possible interactions in the filling gas. While end effects are not

observable in these measurements, they may become noticeable for the more common case of high efficiency counters where a greater fraction of the interactions occur near the end window. Careful attention to experimental geometry can minimize end and wall effects and ensure that the calculated efficiency is an accurate representation of the true counter efficiency.

References

[1] W. J. Price, *Nuclear radiation detection*, 2nd. ed. (McGraw-Hill Book Co., New York, 1964).

[2] I. L. Fowler and P. R. Tunnicliffe, Rev. Sci. Instr. **21** (1950) 734.

[3] E. R. Mosburg, Jr. and W. M. Murphy, J. Nucl. Energy A/B **14** (1961) 25.

[4] Nuclear Data Sheets (Nat. Acad. Sci./Nat. Res. Council, Washington, D. C., Dec. 1962) 5-2-54.

[5] B. J. Snyder and G. L. Gyorey, Nucleonics **23** (1965) 80.

[6] W. Bothe, Z. Physik **120** (1943) 437; Engl. Transl. AEC-TR-1691.

[7] G. C. Hanna, Nucl. Sci. Eng. **11** (1961) 338.

[8] J. F. Raffle, J. Nucl. Energy A/B **10** (1959) 8.

[9] T. E. Sampson, M. S. Thesis (The University of Michigan, 1966) unpublished.